Universiteit Leiden
The Netherlands

Potentiation of the axis involving pentose phosphate pathway/NADPH oxidase/reactive oxygen species drives higher IL-10 production in monocytes of Sub-Saharan Africans

Ongwe, M.E.B.; Mouwenda, Y.D.; Manurung, M.D.; Heieis, G.; Azimi, S.; Adegnika, A.A.; ... ; Everts, B.

Citation
Ongwe, M. E. B., Mouwenda, Y. D., Manurung, M. D., Heieis, G., Azimi, S., Adegnika, A. A., ... Everts, B. (2024). Potentiation of the axis involving pentose phosphate pathway/NADPH oxidase/reactive oxygen species drives higher IL-10 production in monocytes of Sub-Saharan Africans. *European Journal Of Immunology*. doi:10.1002/eji.202451029

Version:	Publisher's Version
License:	Creative Commons CC BY-NC 4.0 license
Downloaded from:	https://hdl.handle.net/1887/4213060

Note: To cite this publication please use the final published version (if applicable).

Check for updates

European Journal of Immunology Clinical·Basic·Translational

Molecular immunology and signaling

Basic

Research Article

Potentiation of the axis involving pentose phosphate pathway/NADPH oxidase/reactive oxygen species drives higher IL-10 production in monocytes of Sub-Saharan Africans

Madeleine Eunice Betouke Ongwe[1,2,3], *Yoanne D. Mouwenda*[1,2], *Mikhael D. Manurung*[1], *Graham Heieis*[1], *Shohreh Azimi*[1], *Ayola A. Adegnika*[1,2,4,5], *Peter G. Kremsner*[2,4], *Taco W. Kuijpers*[6,7], *Maria Yazdanbakhsh*[1] and *Bart Everts*[1]

[1] Leiden University Center of Infectious Diseases, Leiden University Medical Center, Leiden, the Netherlands
[2] Centre de Recherches Médicales de Lambaréné, Lambaréné, Gabon
[3] Institut de Recherches en Écologie Tropicale, Centre National de la Recherche Scientifique et Technologique, Libreville, Gabon
[4] Institut für Tropenmedizin, Eberhard-Karls-Universität Tübingen, Tübingen, Germany
[5] German Center for Infection Research, Tübingen, Germany
[6] Sanquin Research, and Landsteiner Laboratory, Academic Medical Center, University of Amsterdam, Amsterdam, the Netherlands
[7] Emma Children's Hospital, Academic Medical Center, Dept of Paediatric Immunology, Rheumatology and Infectious Diseases, University of Amsterdam, Amsterdam, the Netherlands

Cellular metabolism is a key determinant of immune cell function. Here we found that CD14$^+$ monocytes from Sub-Saharan Africans produce higher levels of IL-10 following TLR-4 stimulation and are bioenergetically distinct from monocytes from Europeans. Through metabolomic profiling, we identified the higher IL-10 production to be driven by increased baseline production of NADPH oxidase-dependent reactive oxygen species, supported by enhanced pentose phosphate pathway activity. Together, these data indicate that NADPH oxidase-derived ROS is a metabolic checkpoint in monocytes that governs their inflammatory profile and uncovers a metabolic basis for immunological differences across geographically distinct populations.

Keywords: Monocytes · ROS · Pentose phosphate pathway · NADPH-oxidase · IL-10

Additional supporting information may be found online in the Supporting Information section at the end of the article.

Correspondence: Maria Yazdanbakhsh and Bart Everts
e-mail: m.yazdanbakhsh@lumc.nl; b.everts@lumc.nl

Maria Yazdanbakhsh and Bart Everts These authors contributed equally to this study.

© 2024 The Author(s). *European Journal of Immunology* published by Wiley-VCH GmbH.

This is an open access article under the terms of the Creative Commons Attribution-NonCommercial License, which permits use, distribution and reproduction in any medium, provided the original work is properly cited and is not used for commercial purposes.

Introduction

Adaptation of immune responses that are known to vary between human populations from different geographical regions is driven by both genetic and environmental factors [1, 2]. Among the immune cell populations that have been shown to be functionally different between populations are monocytes, as evidenced by altered baseline activation marker expression and subset distribution [3], TLR responsiveness [4], and susceptibility to viral infection [5]. Monocytes are central players in the immune response by contributing to the initiation and resolution of inflammation [6]. Monocytes can be attracted by various signals including those derived from pathogens and commensals, and can traffic to the site of inflammation, and produce both inflammatory and anti-inflammatory cytokines to shape local and systemic inflammatory responses [7, 8]. Mapping molecular features that underlie the inflammatory profiles of monocytes, may help identify novel pathways that can be targeted to modulate their function to treat disease.

There is a growing appreciation that monocyte activation, pro- and anti-inflammatory cytokine production, and induction of trained immunity, are associated with, and dependent on, rewiring of cellular metabolic pathways [9–12]. Here, we characterized the immunometabolic phenotype of monocytes of healthy adults from Europeans and Sub-Saharan Africans living in the Netherlands and Gabon, respectively, two populations we previously described to have distinct immune profiles [13]. We found clear differences in the core metabolic pathways between $CD14^+$ monocytes from the two groups. Immunological and in-depth metabolic characterization of the monocytes revealed that monocytes from African donors produced higher levels of the anti-inflammatory cytokine IL-10 upon TLR4 stimulation and had higher baseline NADPH-oxidase activity. Furthermore, we identified elevated NADPH oxidase-derived ROS, fuelled by increased pentose phosphate pathway activity, as the main driver of the enhanced IL-10 production by monocytes from Africans. These findings establish a novel functional link between immunometabolic differences and anti-inflammatory profiles of monocytes, and as such provide important new insights into the molecular mechanisms underlying the differences in inflammatory immune profiles observed between populations from Europe and Sub-Saharan Africa.

Results

Within PBMCs from Africans and Europeans, monocytes show the greatest divergence in metabolism

To explore whether there are baseline metabolic differences in $CD14^+$ monocytes between Africans and Europeans, we analyzed the core metabolic pathway activity in unstimulated $CD14^+$ monocytes isolated from peripheral blood mononuclear cells (PBMCs) from healthy Gabonese and Dutch adults, respectively (the main study population characteristics can be found in Table S1), using real-time extracellular flux analysis (Fig. 1A). Monocytes from Europeans were found to have significantly higher oxygen consumption rates (OCR), as a measure for mitochondrial oxidative phosphorylation (OXPHOS), compared with Africans, both in terms of baseline and ATP-coupled respiration, spare respiratory capacity and maximum mitochondrial respiration (Fig. 1B), indicating overall higher mitochondrial respiratory activity. In contrast, no significant differences were observed in extracellular acidification rate (ECAR) as a measure of glycolysis, between the two groups (Fig. 1C). Of note, the bioenergetic differences in total PBMCs between the two groups (Fig. 1D and Supporting information Fig. S1), were mirrored by the bioenergetic profiles of the monocytes, with a similarly higher baseline respiration in Europeans compared with Africans but with no significant difference in glycolytic parameters (Fig. 1E). This suggests that within the PBMCs of Africans and Europeans, the monocytes display the most profound bioenergetics differences and that the metabolic differences observed in the PBMCs as a whole, are a direct reflection of differences in monocyte metabolism (Supporting information Fig. S2). Of note, this is not a consequence of higher frequencies of $CD14^+$ monocytes in Africans, as these cells were present at lower frequencies in PBMCs from Africans compared with Europeans (Supporting information Fig. S3).

We next assessed whether these differences in core metabolism were associated with an altered functional profile in isolated monocytes. Upon stimulation with TLR4 ligand LPS, $CD14^+$ monocytes from African donors, produced significantly higher levels of anti-inflammatory IL-10 compared with those from Europeans, while the opposite was true for proinflammatory cytokine TNF (Fig. 1F). Within each cohort there was no difference in IL-10 production between male and female, nor was it affected by age (data not shown). No differential expression of proinflammatory cytokines IL-1b or IL-6 was observed (Fig. 1F). This suggests that monocytes from Africans are both metabolically and functionally distinct from those of Europeans, characterized by a more anti-inflammatory profile.

Monocytes from Africans display reduced mitochondrial metabolism compared with Europeans

To start addressing whether the differences in monocyte metabolism between Africans and Europeans could explain the divergence in their inflammatory profile, we performed a more in-depth metabolic characterization and comparison of the $CD14^+$ monocytes from both groups. Flow cytometry-based analysis of mitochondrial membrane potential and mass revealed no differences in the former, but a higher signal of the latter in monocytes from Africans, which may indicate that the lower OXPHOS in monocytes from Africans reflects reduced activity, rather than being a consequence of reduced mitochondrial content (Fig. 2A). Additionally, higher mitochondrial mass was not a consequence of increased cell size because that was comparable for monocytes from Africans and Europeans as determined by forward-scatter

© 2024 The Author(s). European Journal of Immunology published by Wiley-VCH GmbH.

15214141, 2024, 9, Downloaded from https://onlinelibrary.wiley.com/doi/10.1002/eji.202451029, Wiley Online Library on [24/04/2025]. See the Terms and Conditions (https://onlinelibrary.wiley.com/terms-and-conditions) on Wiley Online Library for rules of use; OA articles are governed by the applicable Creative Commons License

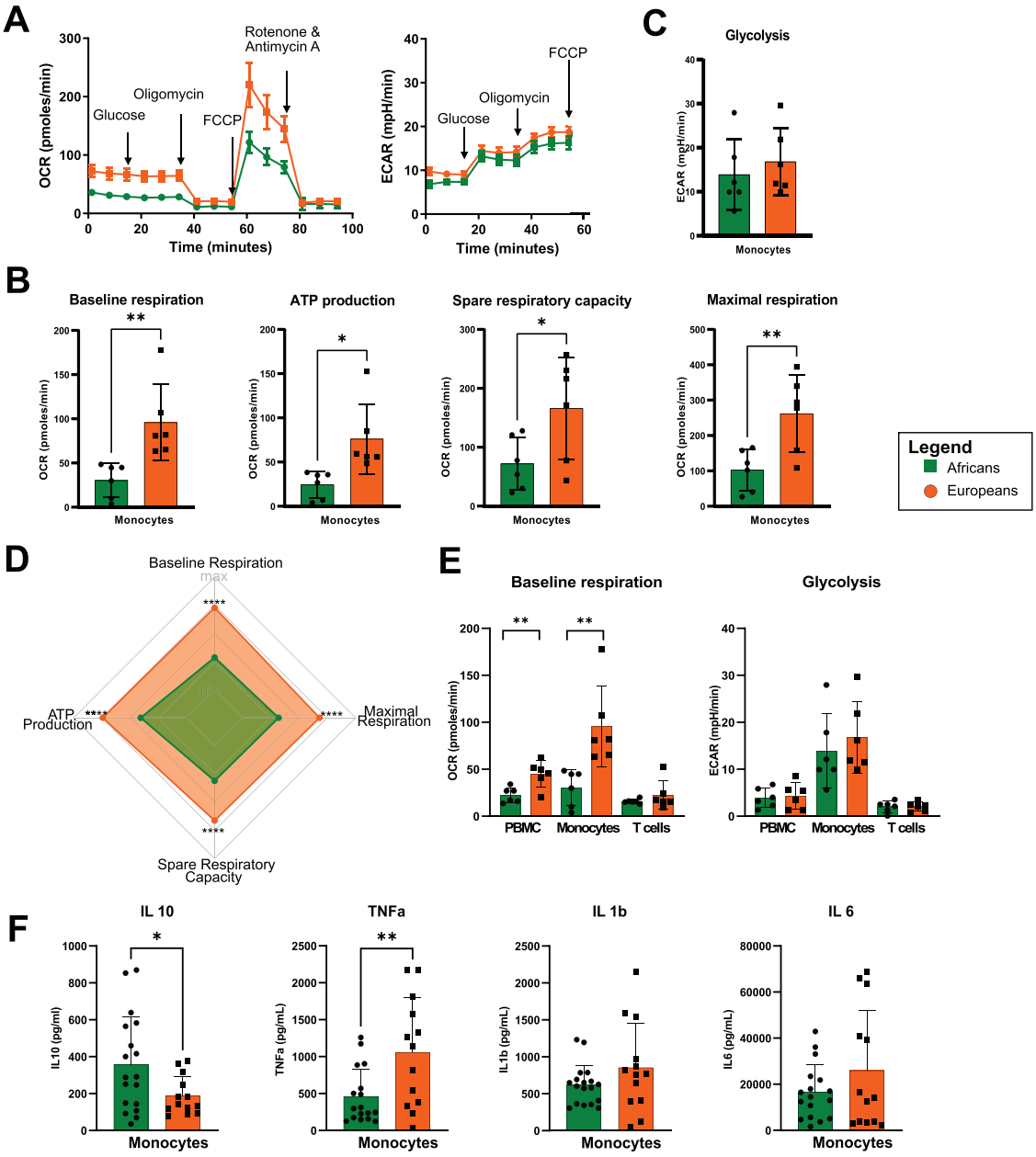

Figure 1. Monocytes from Africans have a distinct bioenergetic and cytokine profile compared with monocytes from Europeans. (A) Oxygen consumption rate (OCR) and extracellular acidification rate (ECAR) were determined in live CD14$^+$ monocytes of Europeans and Africans using the seahorse XF analyzer. A representative plot of a glucose and mitochondrial stress test. (B) Based on a mitochondrial stress test, baseline respiration, ATP production, spare respiratory capacity, and maximal mitochondrial respiration were determined in monocytes. (C) Based on the glycolysis stress test baseline, glycolytic rates of CD14$^+$ monocytes were determined (D) Based on mitochondrial stress test, baseline respiration, ATP production, spare respiratory capacity, and maximal mitochondrial respiration were determined in PBMCs. (E) Baseline respiration (OCR) and glycolysis (ECAR) of CD14$^+$ monocytes and CD4$^+$ T cells isolated from total PBMCs. (F) IL-10, TNFα, IL-1β, IL-6 production by monocytes of Europeans and Africans after LPS stimulation as determined by ELISA in culture supernatants. Bars represent mean ± SD; each dot represents one individual. $^*p < 0.05$, $^{**}p < 0.01$, $^{***}p < 0.001$, $^{****}p < 0.0001$ for significant differences between Europeans and Africans based on unpaired Student's *T*-test.

width (Fig. 2B). Indeed, spectral flow cytometry-based analysis of protein expression of mitochondrial electron transport chain complexes, succinate dehydrogenase A and cytochrome C [14, 15], showed no reduced expression in African monocytes (Fig. 2C). On the other hand, we did observe reduced expression of Carnitine Palmitoyltransferase, a rate limiting transporter required for mitochondrial long chain fatty acid oxidation, in African monocytes (Fig. 2C), hinting toward lower fatty acid oxidation, which could in part explain the reduced OXPHOS in these cells. Consistent with comparable glycolytic rates (Fig. 1C and D), uptake of fluorescent glucose analog 2NBDG by monocytes, was not different between the groups (Fig. 2D), nor was there a difference in expression of rate-limiting enzyme in glycolysis, pyruvate kinase, or glucose transporter (Fig. 2D).

© 2024 The Author(s). *European Journal of Immunology* published by Wiley-VCH GmbH.

15214141, 2024, 9, Downloaded from https://onlinelibrary.wiley.com/doi/10.1002/eji.202451029, Wiley Online Library on [24/04/2025]. See the Terms and Conditions (https://onlinelibrary.wiley.com/terms-and-conditions) on Wiley Online Library for rules of use; OA articles are governed by the applicable Creative Commons License

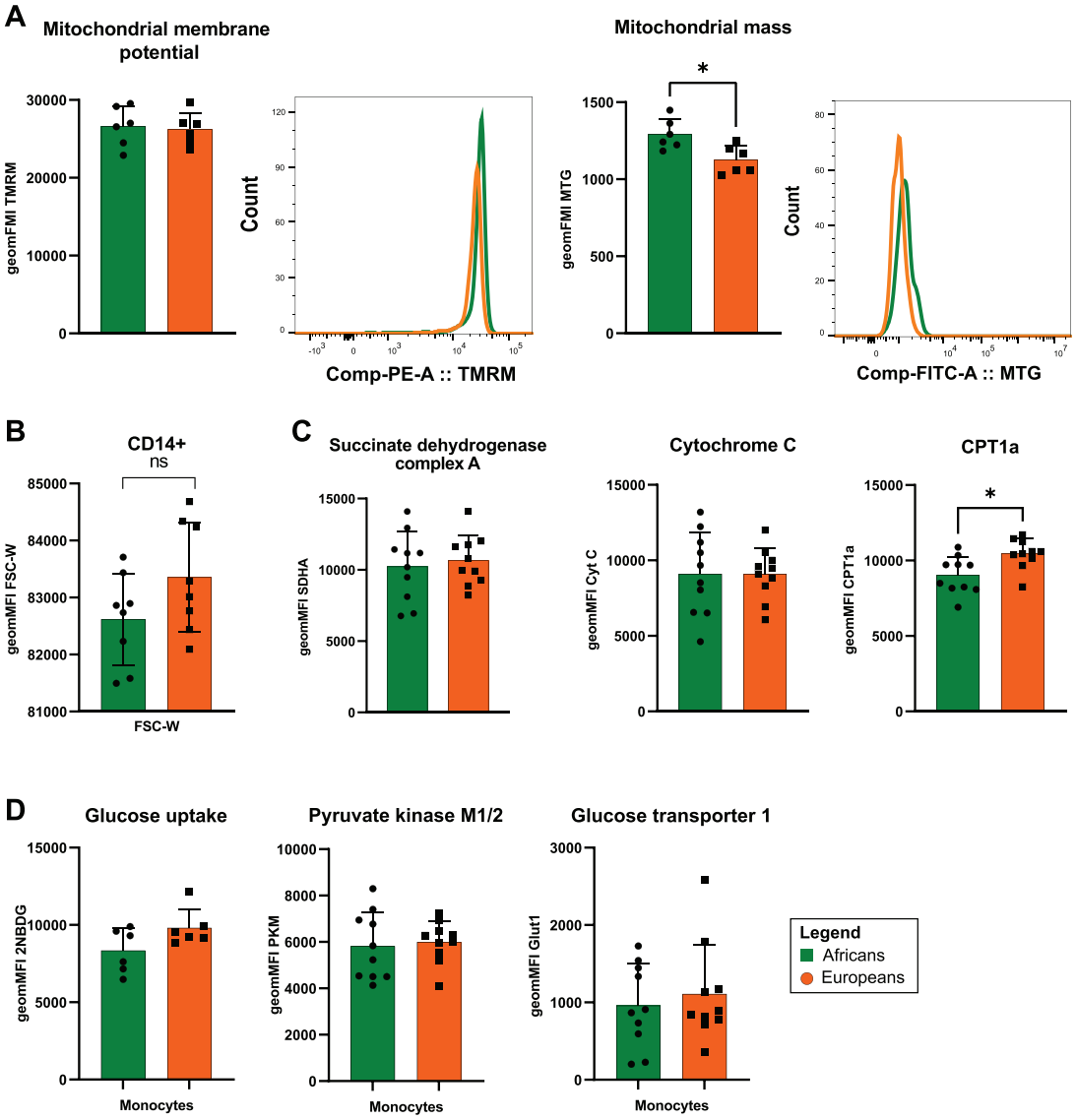

Figure 2. Monocytes from Africans display reduced mitochondrial metabolism at a steady state. (A) Geometric mean fluorescence (geomMFI) of Tetramethyl rhodamine (TMRM) and MitoTracker green (MTG), parameters of mitochondrial membrane potential and mitochondrial mass, respectively, were recorded for isolated $CD14^+$ monocytes from Europeans and Africans using flow cytometry. The histogram shows one representative example of the TMRM and MTG staining. (B) The monocyte size of Europeans and Africans was measured by the mean of forward scatter width (FSC-W). (C) GeomMFI of succinate dehydrogenase A (SDHA) and cytochrome C (CytC), carnitine palmitoyl transferase (CPT1a); and (D) pyruvate kinase 1/2 (PKM) and glucose transporter (Glut1) of Europeans and Africans determined by spectral flow cytometry. Bars represent mean ± SD; each dot represents one individual. $^*p < 0.05$, for significant differences between Europeans and Africans based on unpaired Student's *T*-test.

To further expand these findings, quantitative untargeted metabolomics was performed on monocytes from both groups. A differential analysis showed that 178 out of 277 annotated metabolites were significantly different between Africans and Europeans (Table S1). Among them, 93 metabolites were upregulated in Europeans whereas 85 metabolites were upregulated in Africans (Fig. 3A). Unsupervised clustering analysis of these metabolites revealed distinct clustering patterns among African and European donors. This differentiation was primarily attributed to two sets of clusters representing metabolite abundances in monocytes from the respective study groups. Cluster 1 exhibited metabolites that were more abundant in Europeans, while cluster 2 consisted of metabolites that were more abundant in Africans. (Fig. 3B). Several metabolic pathways were significantly enriched in cluster 1, in particular, those related to amino acids such as alanine, arginine, glutamine, and valine (Fig. 3C and D). In addition, cluster 1 was also significantly enriched for TCA cycle metabolites including acetyl-CoA, itaconate, succinate, fumarate, and malate (Fig. 3C–E). Conversely, tyrosine metabolism was the only metabolic pathway significantly enriched in Cluster 2 (Fig. 3C). This corresponded with a higher concentration of dopamine, of which tyrosine is the precursor, in monocytes from Africans (Fig. 3F). Unbiased metabolic network topology analysis based on the differential abundance of

© 2024 The Author(s). *European Journal of Immunology* published by Wiley-VCH GmbH.

15214141, 2024, 9, Downloaded from https://onlinelibrary.wiley.com/doi/10.1002/eji.202451029, Wiley Online Library on [24/04/2025]. See the Terms and Conditions (https://onlinelibrary.wiley.com/terms-and-conditions) on Wiley Online Library for rules of use; OA articles are governed by the applicable Creative Commons License

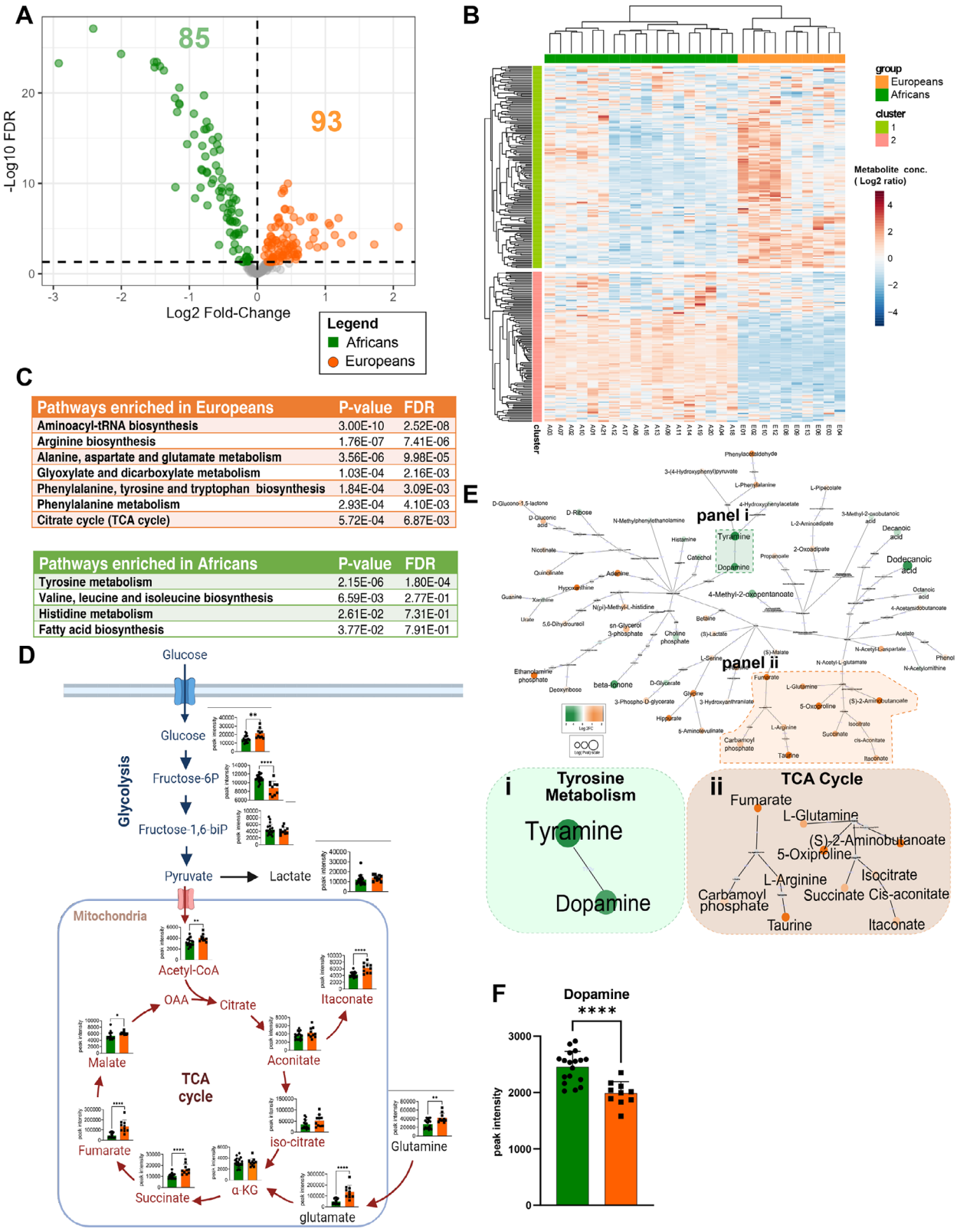

Figure 3. Untargeted metabolomics reveals differential metabolite network enrichment in monocytes from Africans and Europeans. Quantitative LC-MS-based metabolomics was performed on monocyte lysates from Africans and Europeans. (A) A volcano plot of 277 metabolites in which green and orange metabolites indicate the ones that are significantly upregulated in Africans (n = 85) or Europeans (n = 93), respectively. p-values were corrected for false discovery rate (FDR) and the FDR is set at 0.05 level. (B) A heatmap representing an unsupervised clustering analysis of differentially abundant metabolites (rows) from panel (a) comparing African and European subjects (columns). The color of the heatmap tiles

© 2024 The Author(s). *European Journal of Immunology* published by Wiley-VCH GmbH.

15214141, 2024, 9, Downloaded from https://onlinelibrary.wiley.com/doi/10.1002/eji.202451029, Wiley Online Library on [24/04/2025]. See the Terms and Conditions (https://onlinelibrary.wiley.com/terms-and-conditions) on Wiley Online Library for rules of use; OA articles are governed by the applicable Creative Commons License

total metabolites, confirmed reduced TCA cycle metabolites and increased tyrosine metabolism as key metabolic features discriminating African from European monocytes (Fig. 3E). Difference in abundance of metabolites linked to glycolysis were less uniform (Fig. 3D). While glucose and lactate levels were significantly higher in Europeans, the opposite was true for glucose/fructose-6P suggesting a possibly enhanced diversion of carbons from glycolysis into an ancillary pathway such as the pentose phosphate pathway (PPP) in monocytes from Africans. However, due to technical limitations, PPP intermediates could not be detected to substantiate this idea. Overall, these data suggest that ex vivo monocytes from Africans are metabolically distinct from their European counterparts, with lower activity in mitochondrial TCA cycle and respiration as well as in overall amino acid metabolism, but with upregulation of tyrosine metabolism as a notable exception, while overall glycolytic rates appear not to significantly differ.

NADPH oxidase-derived ROS fuelled by the pentose phosphate pathway underpins enhanced IL-10 production in monocytes from Africans

In myeloid cells, ROS, in particular those generated in the mitochondria, have been shown to be an important regulator of IL-10 expression upon TLR stimulation [16]. This prompted us to assess ROS levels in the monocytes from both groups. Whereas no differences were found in steady-state mitochondrial ROS production by monocytes between Africans and Europeans (Fig. 4A), assessment of total cellular ROS levels at baseline revealed a significantly higher abundance in African monocytes compared with those from Europeans, which was retained following LPS stimulation (Fig. 4B). Next, to assess the functional relevance of these findings, we used the ROS scavengers, N-acetyl-cysteine (NAC) and mitoquinone (MQ), to neutralize total or mitochondrial ROS, respectively. Importantly, pretreatment with NAC resulted in a profound decrease in LPS-induced IL-10 production by monocytes from Africans, while MQ had only a modest effect. In contrast, none of these effects were observed in monocytes from Europeans (Fig. 4C). This points toward a key role for non-mitochondrial ROS in promoting increased IL-10 production in monocytes from Africans.

A main source of non-mitochondrial ROS in myeloid cells is NADPH oxidase which uses NADPH and oxygen as substrates to generate ROS [17]. We found a higher expression of a subunit of NADPH oxidase, NOX2, in monocytes from Africans (Fig. 4D). Moreover, when monocytes were treated with a NADPH oxidase inhibitor, diphenyleneiodonium chloride (DPI), we found a significant reduction of total ROS levels. In contrast, total ROS levels were unaffected by antimycin A plus rotenone treatment, which inhibits mitochondrial ROS production originating from Complex III and I from the electron transport chain (Fig. 4E), strongly suggesting that NADPH oxidase is the main source of increased total ROS levels in these cells. Indeed, inhibition of NADPH oxidase with DPI strongly decreased IL-10 production by monocytes from Africans and much less so by those from Europeans (Fig. 4F). This effect appeared to be specific for IL-10 in monocytes from Africans, as TNF production by these cells was not affected by NADPH oxidase inhibition in Africans (Supporting information Fig. S5).

The oxidative branch of the PPP, malic enzyme 1, and isocitrate dehydrogenase 1 are considered three main cellular sources of NADPH, of which particularly the former has been linked to supplying this substrate for NADPH oxidase [18]. In line with this, NADPH levels (Fig. 4G) as well as enzymatic activity of glucose-6-phosphate dehydrogenase (G6PD), a rate-limiting enzyme of the PPP (Fig. 4H), were significantly higher in monocytes from Africans compared with Europeans. Finally, we assessed the functional relevance of this increased PPP activity in regulating IL-10 production by monocytes, and we found that 6-aminonicotinamide, an inhibitor of the PPP, significantly decreased IL-10 production following LPS stimulation in both groups, with the strongest effects on the African monocytes (Fig. 4I). Together, these findings identify ROS derived from enhanced NADPH oxidase activity, fuelled by the PPP in African monocytes as the mechanism that underlies their potentiated IL-10-producing capacity.

NADPH oxidase-derived superoxide underpins IL-10 production in monocytes from Africans by controlling transcription

To further verify that ROS promotes IL-10 in monocytes from Africans, we tested whether boosting accumulation of ROS would be sufficient to enhance IL-10 production and if so which particular types of ROS would be required for that. NADPH oxidase produces superoxide, which is converted by superoxide dismutase (SOD) into hydrogen peroxide (H_2O_2), that in turn is further detoxified into H_2O by catalase. While monocytes from Europeans did not display enhanced LPS-induced IL-10 production following exposure to H_2O_2 or a catalase inhibitor (AT, 3-amino-2,3,4-triazole) to promote accumulation of endogenous H_2O_2, they did following treatment with SOD1 inhibitor, 2-methoxyestradiol (2-ME) (Fig. 5A) which enhanced superoxide accumulation (Fig. 5B). This indicated that only the short-lived

represents the log2 ratio of a metabolite concentration (Conc.) between Africans and Europeans. (C) Tables of the top pathways enriched in Africans and Europeans. Metabolites with HMDB identification number (HMDB ID) that are upregulated in Africans (cluster 2) and Europeans (cluster 1) described in Fig. 3B were loaded in MetaboAnalyst 5.0. (D) Metabolite levels (ion mean intensity) within the indicated core metabolic pathway. (E) Metabolic network topology of metabolites with differential abundance in monocytes from Africans and Europeans in which *p*-value (log (Pval) scale) and log2 fold change (log2FC) of metabolites are indicated. (F) Level of dopamine in monocyte lysates from Africans and Europeans. Bars represent mean ± SD; each dot represents one individual. $^{*}p < 0.05$, $^{**}p < 0.01$, $^{***}p < 0.001$, $^{****}p < 0.0001$ for significant differences between Europeans and Africans based on unpaired Student's *T*-test.

© 2024 The Author(s). *European Journal of Immunology* published by Wiley-VCH GmbH.

15214141, 2024, 9, Downloaded from https://onlinelibrary.wiley.com/doi/10.1002/eji.202451029, Wiley Online Library on [24/04/2025]. See the Terms and Conditions (https://onlinelibrary.wiley.com/terms-and-conditions) on Wiley Online Library for rules of use; OA articles are governed by the applicable Creative Commons License

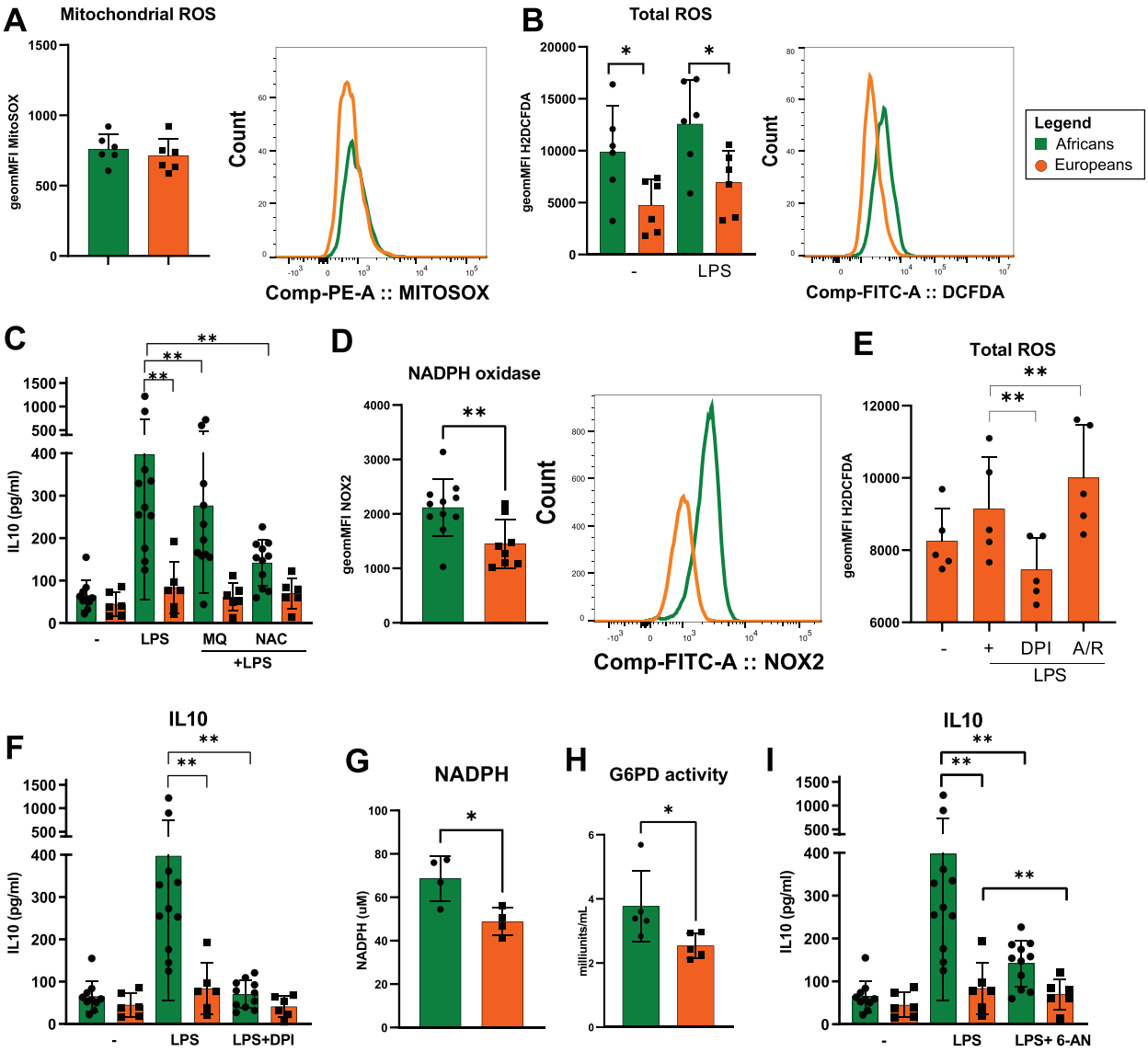

Figure 4. NADPH oxidase-derived ROS fuelled by PPP underpins IL-10 production by monocytes from Africans. (A) Level of mitochondrial ROS measured in CD14+ monocytes of Africans and Europeans at steady state by flow cytometry using the MitoSOX dye. The histogram shows one representative example of MitoSOX staining. (B) Level of Total ROS measured by flow cytometry using H2DCFDA in monocytes of both groups at steady state after LPS stimulation. The histogram shows one representative example of H2DCFDA staining at a steady state in Africans and Europeans. (C) IL-10 production after LPS stimulation in both groups in the presence or absence of mitochondrial ROS scavenger (MQ) and cytoplasmic ROS scavenger (NAC). (D) NADPH oxidase 2 (NOX2) expression was measured by flow cytometry for both groups at steady state. Histogram is one representative example of NOX2 staining. (E) Level of total ROS with and without a pretreatment with NADPH oxidase inhibitor (DPI) or inhibitors of mitochondrial ROS, antimycin A and rotenone (A/R). (F) IL-10 production after LPS stimulation in both groups with or without a pretreatment with DPI. (G) Measurement of NADPH concentration and (H) G6PD activity at steady state in monocytes of both groups. (I) IL-10 production in the presence or absence of pentose phosphate pathway inhibitor (6-AN). Bars represent mean ± SD; each dot represents one individual. $^{*}p < 0.05$, $^{**}p < 0.01$, $^{***}p < 0.001$, $^{****}p < 0.0001$ for significant differences between Europeans and Africans based on unpaired Student's *T*-test. DPI: diphenyleneiodonium; A/R: antimycin A / rotenone; MQ: mitoquinone; NAC: N-acetyl-cysteine.

and highly reactive NADPH oxidase-derived superoxide, but not other ROS such as hydrogen peroxide accumulation, is promoting IL-10 production by monocytes.

Finally, we aimed to determine how ROS controls IL-10 expression. Given the known role of ROS in regulating the function of several transcription factors, such as NF-kB that downstream of TLR4 signaling controls IL-10 expression [19, 20], we hypothesized that NADPH oxidase-derived ROS affects IL-10 expression at the transcriptional level. We found that LPS-induced IL-10 mRNA expression was significantly decreased in the presence of DPI in Africans but not in Europeans (Fig. 5C), indicating that NADPH oxidase activity regulates IL-10 expression transcriptionally in monocytes from Africans. Together, these data suggest the enhanced ability of monocytes from Africans to produce IL-10 following TLR stimulation is dependent on NADPH-oxidase-derived superoxide by acting on transcription.

© 2024 The Author(s). *European Journal of Immunology* published by Wiley-VCH GmbH.

15214141, 2024, 9, Downloaded from https://onlinelibrary.wiley.com/doi/10.1002/eji.202451029, Wiley Online Library on [24/04/2025]. See the Terms and Conditions (https://onlinelibrary.wiley.com/terms-and-conditions) on Wiley Online Library for rules of use; OA articles are governed by the applicable Creative Commons License

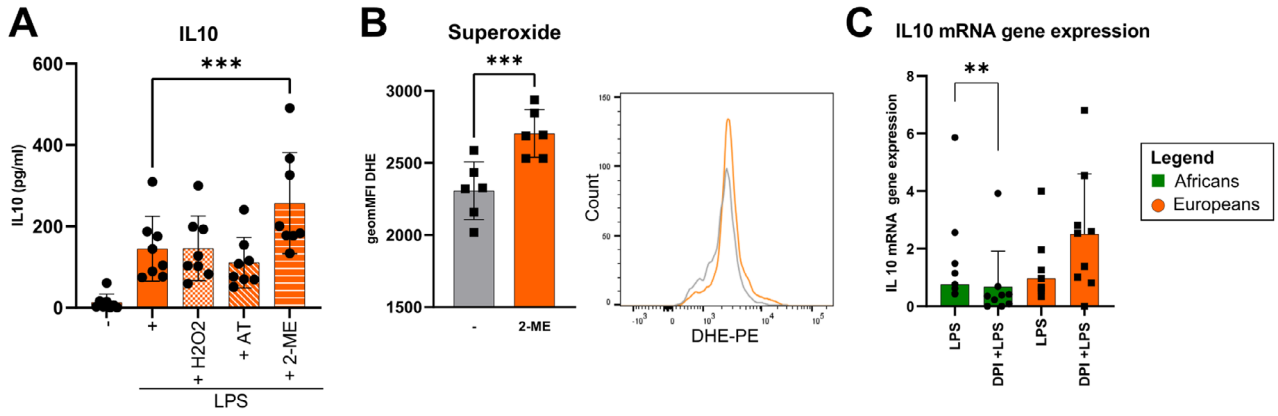

Figure 5. NADPH oxidase-derived superoxide boosts IL-10 production in Europeans and regulates IL-10 transcriptionally. (A) IL-10 production by European monocytes following LPS stimulation in the presence of ROS generators, 2-ME, AT, and H_2O_2. (B) Superoxide production in European monocytes in the absence (in grey) and in the presence (in orange) of 2-methoxyestradiol (2-ME) treatment as determined by flow cytometry using dihydroethidium (DHE), a superoxide dye. The histogram shows one representative example of DHE staining. (C) IL-10 mRNA gene expression in LPS-stimulated monocytes in the presence or absence of DPI in Africans and Europeans. Bars represent mean ± SD; each dot represents the value of one individual. Paired Student's T test was performed to assess significant differences within European or African groups. $^{**}p < 0.01$, $^{***}p < 0.001$. DPI: diphenyleneiodonium; 2-ME: 2-methoxyestradiol; AT: 3-amino-2,3,4-triazole.

Discussion

Here we have found that the monocytes of Africans living in Gabon, produced higher levels of IL-10, an anti-inflammatory cytokine, upon TLR4 stimulation, compared with Europeans. They have higher baseline NADPH oxidase activity and we provide evidence that elevated NADPH oxidase-derived ROS is the main driver of the higher IL-10 production by monocytes from Africans.

An in-depth metabolic comparison of monocytes isolated from Africans and Europeans revealed striking differences in their metabolic profile at baseline. First, we found that at steady state, monocytes from Africans display reduced OXPHOS despite having neither apparent defects in electron transport chain protein expression, nor loss of mitochondrial mass. Furthermore, these cells displayed lower concentrations of TCA cycle substrates and intermediates, suggesting an overall decrease in mitochondrial activity. Interestingly, this was not mirrored by an increase in glycolysis, indicating that these cells have reduced ATP turnover and are more bioenergetically quiescent compared with their Europeans counterparts. Indeed, a significant decrease in aminoacyl-tRNA biosynthesis, a crucial step in protein synthesis and one of the most energy-consuming processes in cells [21], was lower in the monocytes of Africans, while Europeans showed a significant enrichment in this process (Fig. 3C). However, the causal relationship and potential immunological implications of these findings remain to be determined. Among the TCA intermediates that were present at higher concentrations in monocytes from Europeans than from Africans were succinate and α-ketoglutarate, two metabolites that have been shown to have the potential to affect the balance in pro- and anti-inflammatory cytokine production by myeloid cells. Succinate can promote IL-1β expression following TLR stimulation by supporting HIF-1α stabilization [22]. However, we did not find differences in IL-1β expression between the two groups, suggesting that IL-1β expression following TLR stimulation in monocytes is not affected by differences in baseline succinate levels. α-ketoglutarate can epigenetically promote the expression of anti-inflammatory genes, including IL-10 [23] by regulating the activity of Jumonji C domain-containing histone demethylases [24]. However, given that we found high IL-10-expressing African monocytes to have comparable α-ketoglutarate levels to Europeans, it is unlikely that the differential abundance of α-ketoglutarate between the two groups is an important driver of the differences in IL-10 expression.

Secondly, monocytes from Africans displayed a clearly distinct, but mostly lower amino acid metabolism. Studies in rheumatoid arthritis patients have revealed that the proinflammatory phenotype of monocytes is dependent on an increased ability to take up amino acids [25], which makes it conceivable that the differences in amino acid metabolism between monocytes from the two populations contribute to their distinct inflammatory profiles. One notable exception to the overall lower levels of metabolism of amino acids in African monocytes was that of tyrosine, which was significantly increased. This was associated with increased concentrations of dopamine, of which tyrosine is the main precursor. Although dopamine is well-known for its neurological effects, it also modulates immune cell function, including that of myeloid cells. Dopamine has been shown to reduce TNF but increase IL-10 production following LPS stimulation of human macrophages [26], which warrants further study into exploring the contribution of dopamine in the differences we observed in the inflammatory status of monocytes.

Finally, we found significantly elevated cytoplasmic ROS levels in monocytes from Africans compared with Europeans which we identified to be derived from increased NADPH oxidase activity. Furthermore, our data provide support for increased baseline PPP activity in African monocytes, presumably to provide NADPH to fuel enhanced NADPH oxidase activity both prior to and upon cellular activation. Most importantly, we demonstrated a critical role for this pathway in underpinning the heightened IL-10 production by African monocytes, as neutralizing cytoplas-

© 2024 The Author(s). *European Journal of Immunology* published by Wiley-VCH GmbH.

15214141, 2024, 9, Downloaded from https://onlinelibrary.wiley.com/doi/10.1002/eji.202451029, Wiley Online Library on [24/04/2025]. See the Terms and Conditions (https://onlinelibrary.wiley.com/terms-and-conditions) on Wiley Online Library for rules of use; OA articles are governed by the applicable Creative Commons License

15214141, 2024, 9, Downloaded from https://onlinelibrary.wiley.com/doi/10.1002/eji.202451029, Wiley Online Library on [24/04/2025]. See the Terms and Conditions (https://onlinelibrary.wiley.com/terms-and-conditions) on Wiley Online Library for rules of use; OA articles are governed by the applicable Creative Commons License

mic ROS either through blocking NADPH oxidase or PPP activity reduced LPS-induced IL-10 secretion selectively in African monocytes. ROS generated by NADPH oxidase is most well-known for playing an important role in host antimicrobial defense. In addition, induction of NADPH oxidase activity following activation of macrophages [27], monocytes [28], and HEK293 cells [29], has been shown to support proinflammatory cytokine responses by these cells. Our findings indicate that in Africans, monocytes increased NADPH-oxidase activity and ROS levels, already prior to stimulation, may have a different outcome and instead control IL-10 expression rather than proinflammatory cytokines upon subsequent activation. Indeed, preincubation of European monocytes with a SOD inhibitor significantly boosted superoxide accumulation in the cells and was sufficient to boost their IL-10 production following LPS stimulation. This would be largely consistent with a study showing that chronic exposure to ROS in the context of kidney disease, resulted in increased IL-10 production by monocytes [30] and conversely monocytes from chronic granulomatous disease patients, that have functional defects in NADPH oxidase, displayed reduced IL-10 production but not proinflammatory cytokines upon LPS stimulation [31].

We found that LPS-induced IL-10 mRNA expression was significantly decreased when NADPH oxidase was inhibited in African monocytes, indicating that ROS transcriptionally regulates IL-10 production. Yet, how ROS derived from NADPH oxidase promotes IL-10 mRNA expression in African monocytes remains to be addressed. Key regulators of IL-10 transcription are NF-kB subunits BCL3 and p50, CREB, and transcription factors SP1 and 3 downstream of MAP kinase p38 [32–34], and their activity or expression have been shown to be ROS sensitive [19, 20, 35-37]. Of note, in these studies primarily H_2O_2 has been shown to act on these targets, while in our hands superoxide but not H_2O_2 was capable of promoting IL-10 expression in monocytes. Further studies are required to determine if and how superoxide in monocytes promotes potentiate activity of one or more of these transcription factors to boost IL-10 mRNA expression, without significantly affecting expression of proinflammatory cytokines.

Our immunometabolic data extend previous studies that have documented differences in phenotype at baseline and functional responses following TLR stimulation of monocytes from individuals from Africa compared with Europe [3, 4]. The drivers behind these immunological differences — and as we find in this work — metabolic differences, are likely multifactorial. One such driver is the level of exposure to micro-organisms and parasites which is much higher in African populations compared with those from Europe and is known to have a major impact on the immune system and to promote immune-regulatory networks [38, 39]. Indeed, the immunological phenotype of the monocytes from Africans resembles that of tolerized monocytes that produce low proinflammatory and high anti-inflammatory cytokines upon LPS stimulation following low-grade pre-exposure to LPS [40]. Moreover, metabolically, the altered redox balance, lower levels of OXPHOS, increased PPP [41] and NADPH oxidase activity [42] observed in African monocytes are strikingly similar to those reported in tolerized monocytes in the context of sepsis [43, 44], further supporting the notion that distinct microbial exposure is an important driver of the immunometabolic differences between monocytes from the Africans and Europeans. Apart from differences in microbial exposure, differences in diet and lifestyle between the two groups may also influence the observed immunological differences [45]. For instance, recent work has shown that food-derived metabolites — highly abundant in rural-living individuals from Tanzania compared with those living in urban areas characterized by a Western lifestyle — could account for an anti-inflammatory immune profile observed in those living in rural areas, rather than age, sex, or genetic differences [45]. Finally, apart from these environmental factors, differences in genetics cannot be ruled out [46, 47]. This is illustrated by a study in which oxidative stress levels in cells from Afro-Americans, with genetic ties to West-Central Africa, and Caucasians from the same urban setting were compared [48]. Monocytes from Afro-Americans displayed increased levels of oxidative stress due to higher expression of NADPH oxidase, making it conceivable that differences in baseline NADPH oxidase expression in our two study groups may at least in part have a genetic basis.

In summary, we have uncovered a previously unappreciated role for metabolism in underpinning differences in anti-inflammatory IL-10 production of monocytes from two geographically distinct populations. Although future studies will be needed to validate our findings in more diverse cohorts, they provide potential new leads to modulate monocyte function in the context of combating infectious and chronic inflammatory diseases.

Materials and methods

Sample collection

BMCs were obtained from blood that healthy Dutch residents in the Netherlands donated voluntarily to LUMC Blood Bank. The donated material was processed and analyzed anonymously. PBMCs from healthy Gabonese were collected as part of the HOOKVAC trial (Clinicaltrials.gov ID: NCT02126462) prior to vaccine administration. Written informed consent was obtained from each participant (see Table S1 for participants' characteristics). The collected blood was processed and analyzed anonymously.

Cell isolation

Venous blood of healthy volunteers living in Gabon (Africans) and in the Netherlands (Europeans) was collected in heparin tubes followed by an isolation of PBMCs using 1.0772 Ficoll-Paque density gradient centrifugation. Isolated PBMCs were cryopreserved in 20% fetal bovine serum (lot number 45110321FBS from SERANA) /10% dimethyl sulfoxide/RPMI-1640 complete medium containing 1 mM pyruvate, 2 mM L-glutamine, 100 U/mL penicillin, 10 μg/mL streptomycin (all from Sigma-Aldrich).

© 2024 The Author(s). *European Journal of Immunology* published by Wiley-VCH GmbH.

Cryovials were stored overnight at –80°C in controlled-grade Mr. Frosty Freezing Container (Thermo Scientific, cat: 5100–0001) before transferring to liquid nitrogen for long-term storage until analysis. PBMCs stored in Gabon were shipped to the Netherlands and monocytes were directly isolated from thawed PBMCs from both European and African using CD14 positive selection beads following the manufacturer's instructions (Miltenyi Bioscience) with a purity of >95 % and a viability of >90 % and were directly cultured.

Extracellular flux analysis

Real-time metabolic analysis on PBMCs or isolated monocytes was performed using the XF96e Extracellular Flux analyzer (Agilent) and analyzed using Wave Desktop (Version 2.6, Agilent). Cells were counted and resuspended in pH 7.4 Seahorse media deprived of glucose and plated at 3×10^5 PBMCs or 1.5×10^5 monocytes. The XF cartridge was prehydrated and filled with the following reagents for sequential injection during the run: glucose (10 mM; port A; #G8644-100mL, Sigma), oligomycin (1 μM; port B; #11342, Cayman Chemical), fluoro-carbonyl cyanide phenylhydrazone (3 μM; port C; # C2920-10MG, Sigma), and finally, rotenone/antimycin A (1/1 μM; port D; #R8875-1G/#A8674-25MG, Sigma). OCR and ECAR were recorded. The following metabolic parameters were calculated: Glycolysis rate = increase in ECAR in response to injection A. Glycolytic capacity = increase in ECAR in response to injection A and injection B. Baseline respiration = difference in OCR between readings following port A injection and readings after port D injection. Spare respiratory capacity = difference between baseline respiration and maximum mitochondrial respiration which is calculated based on the difference in OCR between readings following port C injection and readings after port A injection. ATP production = difference in OCR between readings following port A injection and readings after port B injection. At the end of the run XF culture plates, supernatants were carefully discarded, and cells were washed with PBS, lysed in 25 μL of a RIPA-like buffer (50 mM Tris-HCl [pH 7.4], 150 mM NaCl, and 0.5% SDS) and the plate was stored at −20°C for later protein content quantification and normalization for cell input using a bicinchoninic acid protein assay kit (BCA; #PIER23225, Pierce) according to the manufacturer's recommendations. A representative plot of extracellular flux analysis is shown in Fig. 1A.

Culture conditions and cytokine measurements

Monocytes were plated at 1×10^5 cells per well and cultured for 24 h in a total of 200 μL of RPMI 1640 complete medium with TLR4 ligands and/or inhibitors. Ultrapure LPS (*Escherichia coli* 0111 B4 strain, #tlrl-3pelps, Invitrogen) was used at 100 ng/mL for 24 h. Where indicated cells were pretreated for 1 h with the following compounds: 1 μM Oligomycin (Cayman Chemical), 1 μM rotenone/antimycin A (R/A; 1/1, Sigma-Aldrich), 10 mM 2-deoxyglucose (2DG; Sigma-Aldrich), 10 μM DPI (Sigma-Aldrich), 100 μM 6-aminonicotinamide (Sigma-Aldrich), 5 mM NAC (Sigma-Aldrich), 10 MQ (Bio Vision), 10 μM 3-amino-1.2.4-triazole (3-AT; Sigma-Aldrich), 10 μM 2-ME (Sigma-Aldrich), 1 Mm apocycin (APO; Sigma-Aldrich). These compounds were prepared in 100 μL of complete medium at their respective end concentration and added to the monocyte cultures 1 h before LPS stimulation. Subsequently, cells were used for different readouts.

Cytokine production

Stimulated cells were kept for a total of 24 h in a 5% CO_2 and 37°C in the incubator. Supernatants were collected after 24 h and concentrations of IL-10, IL-6, IL-1b, and TNF were determined by ELISA (BD Biosciences) according to the manufacturer's protocol.

Flow cytometry

Thawed PBMCs or isolated $CD14^+$ monocyte suspensions were directly stained with 50 μL of antibody cocktail (Table S2) for 30 min at 4°C, followed by LIVE/DEAD Fixable Aqua dead cell Stain Kit (Invitrogen, cat: L34957) for 15 min in the dark at room temperature (RT). Thereafter, cells were separately stained with 100 μL of following fluorescents metabolic dyes prepared in complete RPMI medium and put at 37°C in incubator for 30 min to assess superoxide levels with 10 μM of dihydroethidium (Sigma-Aldrich), total cellular ROS with 1 μM H2DCFDA (Invitrogen), mitochondrial ROS with 10 μM MitoSOX (Invitrogen), mitochondrial membrane potential with 20 nM of Tetramethyl rhodamine (TMRM, #T668, Invitrogen), mitochondrial mass with 1 μM Mitotracker Green (MitoSOX, #M7514, Invitrogen) and glucose uptake with 2-NBDG (10 μM, Invitrogen). Cells were acquired on BD FACS Canto II flow cytometer (BD Biosciences) and analyzed using FlowJo V10 (Tree Star).

For spectral flow cytometry measurements, thawed PBMCs were stained with LIVE/DEAD Zombie NIR for 15 min in the dark at room temperature followed by a staining with a cocktail of surface markers antibodies (Table S3) for 15 min. Next, cells were fixed with 4% PFA (Thermo Scientific) for 15 min, permeabilized for 30 min, and stained 30 min for a second time with 50 μL of metabolic antibodies cocktail freshly prepared in permeabilization buffer (Table S4). Cells were acquired in a 5-laser Cytek Aurora cytometer together with calibration beads and analyzed using FlowJo V10 (Tree Star). Live $CD14^+$ monocytes were selected following the gating strategy shown in Supporting information Fig. S4 and mean fluorescence intensity of each metabolic marker was recorded within the $CD14^+$ live monocytes.

RNA isolation + RT-qPCR

$CD14^+$ isolated monocytes were harvested after 24 h LPS stimulation w/wo DPI and transferred in 1.5 Eppendorf vial. After three steps of centrifugation/ washing with PBS, the pellet was

© 2024 The Author(s). *European Journal of Immunology* published by Wiley-VCH GmbH.

15214141, 2024, 9, Downloaded from https://onlinelibrary.wiley.com/doi/10.1002/eji.202451029, Wiley Online Library on [24/04/2025]. See the Terms and Conditions (https://onlinelibrary.wiley.com/terms-and-conditions) on Wiley Online Library for rules of use; OA articles are governed by the applicable Creative Commons License

15214141, 2024, 9, Downloaded from https://onlinelibrary.wiley.com/doi/10.1002/eji.202451029, Wiley Online Library on [24/04/2025]. See the Terms and Conditions (https://onlinelibrary.wiley.com/terms-and-conditions) on Wiley Online Library for rules of use; OA articles are governed by the applicable Creative Commons License

put in liquid nitrogen and stored at −80°C until the next day. RNA isolation was performed using NucleoSpin RNA kit (MACHEREY-NAGEL kit, lot 1810/001) according to manufacturer instructions. Right after RNA isolation, cDNA synthesis was done by RT-qPCR. A total of 9 μL of RNA were combined with 11 μL of a mix (4 μL of 5x First-Strand buffer, 2 μL of 0.1 M DTT, 1 μL of RNaseOUT (40 U/μL), 1 μL hexamers/random primers (250 ng/μL), 2 μL dNTPs (6.25 mM each), 1 μL RT (M,MLV, 200 u/μL), all from Invitrogen) following a program of 10 min. at 25°C, 50 min at 37°C and 15 min. at 70°C. Thereafter, RT-PCR was performed with 2 μL of cDNA obtained from each sample and mixed with 8 μL of a mix of H2O, 2x SYBR Green Supermix (ThermoFisher), 20 μM of forward primer and reverse primer of IL-10 (forward: AAGACCCAGACATCAAGGCG, reverse: CAGGGAAGAAATCGATGACAGC from Eurofins Genomics) or the control Beta-2-M (B2M, forward: GCCTGCCGTGTGAACCAT, reverse: GGTTGACTGAAGTTAGCAAGCA from Eurogentec). For RT-PCR, all samples were plated in duplicate, and mean C*t* values were recorded together with their standard deviation for IL10 and B2M. The differential mRNA gene expression for each sample was calculated by delta delta C*t* (ΔΔC*t*) relative to the control B2M and set to 2 ($2^{-\Delta\Delta Ct}$). $\Delta Ct_{(\text{sample A})} = \text{Mean } Ct_{\text{IL10(sample A)}} - Ct_{\text{B2M(sample A)}}$, $\Delta\Delta Ct_{(\text{sample A})} = \text{mean } Ct_{\text{A}} - \Delta Ct_{(\text{sample A})}$.

NADPH quantification

NADPH levels were quantified using 1×10^6 isolated $CD14^+$ monocytes as input using an NADPH colorimetric assay kit (ab186031; Abcam) following the manufacturer's recommendations.

Glucose-6 phosphate dehydrogenase activity

Glucose-6 phosphate dehydrogenase activity was measured using 5×10^5 isolated $CD14^+$ monocytes as input using the glucose-6 phosphate dehydrogenase colorimetric assay kit (catalog number MAK015; Sigma-Aldrich) according to the manufacturer's instructions.

Metabolite extraction and LC-MS metabolomics

Monocyte lysates were extracted at a minimum of 5×10^5 cells in 700 μL of a preheated 70°C extraction solvent (70% ethanol: 7 mL EtOH, 3mL HPLC-grade water) after washing twice the monocyte suspension with a solution containing ammonium carbonate (75 mM, Sigma-Aldrich) and HPLC-grade water, adjusted to pH 7.3–7.5 and kept at 37°C in an incubator. Samples were centrifugated at 14,000 rpm for 10 min at 4°C and 500 μL of the extract supernatant from each centrifugated sample was transferred to a prechilled microtube without disturbing the pellet material. Extract supernatants were stored at −80°C until shipped to General Metabolics LLC in Boston, USA for quantitative metabolomic analysis. Polar metabolites were analyzed according to General Metabolic' high-throughput, nontargeted metabolomics platform in negative ion mode [49]. Each sample was injected twice. Mean ion intensity (m/z) data for each annotated metabolite was provided. A total of 817 metabolites were annotated. Metabolites with above 200 ion m/z were drug-related metabolites and were not considered for the analysis. From the remaining ones (n = 315), only 277 metabolites that have an HMDB identification were considered for differential analysis.

Differential analysis

To analyze the differential abundance of each metabolite between monocytes from Africans and Europeans, we used *limma* R/Bioconductor package on log2-transformed mean ion intensity data using the R statistical software version 4.0.2. For the differential metabolite abundance analysis, false discovery rate (FDR) correction was applied and metabolites with FDR below 0.05 level were considered significant. Visualization of the differential analysis was performed using volcano plot and heatmap, which were generated using ggplot2 and ComplexHeatmap R package, respectively.

Pathway enrichment analysis

Metabolites with HMDB identification that are upregulated in Africans and in Europeans were loaded in MetaboAnalyst 5.0 (https://genap.metaboanalyst.ca/MetaboAnalyst) for pathway analysis. In addition, the results table of the differential analysis, containing *p*-value (FDR = adjusted *p*-value) and log2 fold change (log2FC), was loaded in https://artyomovlab.wustl.edu/shiny/gatom/ to perform pathway analysis (network topology). The network summary built was generated as the .xgmml file. This network file was then imported to Cytoscape 3.9.1 for styling and visualization.

Study approval

The HOOKVAC trial was approved by the national ethical committee of Gabon (#0033/2014/SG/CNE) and done under an investigation new drug application (IND#016184) to the US Food and Drug Administration. Written informed consent was obtained from each participant. Participants found to be infected with parasitic helminths were treated two weeks prior to vaccination (Table S1). Participants of the trial were healthy and free of HIV, hepatitis B, or malaria parasites before vaccination. The trial followed the principle of the Declaration of Helsinki, Good Clinical Practice, and Good Clinical and Laboratory Practice.

Statistical analysis

Data were analyzed for statistical significance using GraphPad Prism 9.3 statistical software (GraphPad Software). Comparison between Africans and Europeans for OCR, ECAR, cytokines, and

© 2024 The Author(s). *European Journal of Immunology* published by Wiley-VCH GmbH.

cytometry data were performed using the paired or unpaired Student's *t*-test. All statistically significant comparisons are annotated using asterisks $*p < 0.05$, $**p < 0.01$, $***p < 0.001$. For significance between Africans and Europeans, we used unpaired student's *T*-test and for significance within each group, we used paired student's *T*-test.

Acknowledgements: This work was funded by a LUMC fellowship (B.E.) and supported by NIH grant (U01A165745). E.B.O. was supported by WISE EDCTP PISA2020AGDG. In addition, this study is part of the EDCTP2 programme supported by the European Union. The funders had no role in study design, data collection and analysis, decision to publish, or preparation of the manuscript.

Conflicts of Interest Statement: The authors declare no financial or commercial conflict of interest.

Author Contributions: Conceptualization, methodology, and formal analysis: Madeleine Eunice Betouke Ongwe, Bart Everts, and Maria Yazdanbakhsh. Software: Madeleine Eunice Betouke Ongwe, Mikhael D. Manurung, Bart Everts. Investigation: Madeleine Eunice Betouke Ongwe, Yoanne D. Mouwenda, and Ayola A. Adegnika. Data curation: Madeleine Eunice Betouke Ongwe and Bart Everts. Visualization: Madeleine Eunice Betouke Ongwe, Mikhael D. Manurung, Bart Everts, and Maria Yazdanbakhsh. Supervision: Bart Everts and Maria Yazdanbakhsh. Validation: Madeleine Eunice Betouke Ongwe and Bart Everts. Project administration: Bart Everts and Maria Yazdanbakhsh. Writing—original draft preparation: Madeleine Eunice Betouke Ongwe. Writing—review and editing: Madeleine Eunice Betouke Ongwe, Yoanne D. Mouwenda, Mikhael D. Manurung, Graham Heieis, Shohreh Azimi, Ayola A. Adegnika, Peter G. Kremsner, Taco W. Kuijpers, Bart Everts, and Maria Yazdanbakhsh.

Data Availability Statement: All data are available in the main text or the supplementary materials.

Peer review: The peer review history for this article is available at https://publons.com/publon/10.1002/eji.202451029.

References

1 **Brodin, P. and Davis, M. M.** Human immune system variation. *Nat. Rev. Immunol.* 2017. **17**: 21–29.

2 **van Dorst, M., Pyuza, J. J., Nkurununngi, G., Kullaya, V. I., Smits, H. H., Hogendoorn, P. C. W., Wammes, L. J. et al.**, Immunological factors linked to geographical variation in vaccine responses. *Nat. Rev. Immunol.* 2023. **24**: 250–263.

3 **Appleby, L. J., Nausch, N., Midzi, N., Mduluza, T., Allen, J. E. and Mutapi, F.** Sources of heterogeneity in human monocyte subsets. *Immunol. Lett.* 2013. **152**: 32–41.

4 **Quach, H., Rotival, M., Pothlichet, J., Loh, Y. E., Dannemann, M., Zidane, N., Laval, G. et al.**, Genetic adaptation and neandertal admixture shaped the immune system of human populations. *Cell*. 2016. **167**: 643–656 e17.

5 **O'Neill, M. B., Quach, H., Pothlichet, J., Aquino, Y., Bisiaux, A., Zidane, N., Deschamps, M. et al.**, Single-cell and bulk RNA-sequencing reveal differences in monocyte susceptibility to influenza A virus infection between Africans and Europeans. *Front. Immunol.* 2021. **12**: 768189.

6 **Austermann, J., Roth, J. and Barczyk-Kahlert, K.** The good and the bad: monocytes' and macrophages' diverse functions in inflammation. *Cells.* 2022. **11**: 1979.

7 **Yang, J., Zhang, L., Yu, C., Yang, X.-F. and Wang, H.** Monocyte and macrophage differentiation: circulation inflammatory monocyte as biomarker for inflammatory diseases. *Biomarker Res*. 2014. **2**: 1.

8 **Shi, C. and Pamer, E. G.** Monocyte recruitment during infection and inflammation. *Nat. Rev. Immunol*. 2011. **11**: 762–774.

9 **Lachmandas, E., Boutens, L., Ratter, J. M., Hijmans, A., Hooiveld, G. J., Joosten, L. A., Fransen, J. A. M. et al.**, Microbial stimulation of different Toll-like receptor signalling pathways induces diverse metabolic programmes in human monocytes. *Nat. Microbiol.* 2016. **2**: 16246.

10 **Zhang, B., Moorlag, S. J., Dominguez-Andres, J., Bulut, O., Kilic, G., Liu, Z., Van Crevel, R. et al.**, Single-cell RNA sequencing reveals induction of distinct trained-immunity programs in human monocytes. *J. Clin Invest.* 2022. **132**: e147719.

11 **Zhu, X., Meyers, A., Long, D., Ingram, B., Liu, T., Yoza, B. K., Vachharajani, V. et al.**, Frontline science: monocytes sequentially rewire metabolism and bioenergetics during an acute inflammatory response. *J. Leukoc Biol*. 2019. **105**: 215–228.

12 **Yamada, K. J., Heim, C. E., Xi, X., Attri, K. S., Wang, D., Zhang, W., Singh, P. K. et al.**, Monocyte metabolic reprogramming promotes pro-inflammatory activity and Staphylococcus aureus biofilm clearance. *PLoS Pathog.* 2020. **16**: e1008354.

13 **de Jong, S. E., van Unen, V., Manurung, M. D., Stam, K. A., Goeman, J. J., Jochems, S. P., Höllt, T. et al.**, Systems analysis and controlled malaria infection in Europeans and Africans elucidate naturally acquired immunity. *Nat. Immunol.* 2021. **22**: 654–665.

14 **Ahl, P. J., Hopkins, R. A., Xiang, W. W., Au, B., Kaliaperumal, N., Fairhurst, A. M. and Connolly, J. E.** Met-Flow, a strategy for single-cell metabolic analysis highlights dynamic changes in immune subpopulations. *Commun. Biol.* 2020. **3**: 305.

15 **Pelgrom, L. R., Patente, T. A., Otto, F., Nouwen, L. V., Ozir-Fazalalikhan, A., van der Ham, A. J., Van Der Zande, H J.P. et al.**, mTORC1 signaling in antigen-presenting cells of the skin restrains CD8(+) T cell priming. *Cell Rep.* 2022. **40**: 111032.

16 **Mills, E. L., Kelly, B., Logan, A., Costa, A. S. H., Varma, M., Bryant, C. E., Tourlomousis, P. et al.**, Succinate dehydrogenase supports metabolic repurposing of mitochondria to drive inflammatory macrophages. *Cell*. 2016. **167**: 457–470 e13.

17 **Canton, M., Sanchez-Rodriguez, R., Spera, I., Venegas, F. C., Favia, M., Viola, A. and Castegna, A.** Reactive oxygen species in macrophages: sources and targets. *Front. Immunol.* 2021. **12**: 734229.

18 **Britt, E. C., Lika, J., Giese, M. A., Schoen, T. J., Seim, G. L., Huang, Z., Lee, P Y. et al.**, Switching to the cyclic pentose phosphate pathway powers the oxidative burst in activated neutrophils. *Nat. Metab*. 2022. **4**: 389–403.

19 **Ndengele, M. M., Muscoli, C., Wang, Z. Q., Doyle, T. M., Matuschak, G. M. and Salvemini, D.** Superoxide potentiates NF-kappaB activation and modulates endotoxin-induced cytokine production in alveolar macrophages. *Shock*. 2005. **23**: 186–193.

20 **Gloire, G., Legrand-Poels, S. and Piette, J.** NF-kappaB activation by reactive oxygen species: fifteen years later. *Biochem. Pharmacol.* 2006. **72**: 1493–1505.

© 2024 The Author(s). *European Journal of Immunology* published by Wiley-VCH GmbH.

15214141, 2024, 9, Downloaded from https://onlinelibrary.wiley.com/doi/10.1002/eji.202451029, Wiley Online Library on [24/04/2025]. See the Terms and Conditions (https://onlinelibrary.wiley.com/terms-and-conditions) on Wiley Online Library for rules of use; OA articles are governed by the applicable Creative Commons License

21 **Buttgereit, F. and Brand, M. D.** A hierarchy of ATP-consuming processes in mammalian cells. *Biochem. J.* 1995. **312**(Pt): 163–167.

22 **Tannahill, G. M., Curtis, A. M., Adamik, J., Palsson-McDermott, E. M., McGettrick, A. F., Goel, G., Frezza, C. et al.**, Succinate is an inflammatory signal that induces IL-1beta through HIF-1alpha. *Nature*. 2013. **496**: 238–242.

23 **Cheng, M. X., Cao, D., Chen, Y., Li, J. Z., Tu, B. and Gong, J. P.** alpha-ketoglutarate attenuates ischemia-reperfusion injury of liver graft in rats. *Biomed. Pharmacother.* 2019. **111**: 1141–1146.

24 **Liu, P. S., Wang, H., Li, X., Chao, T., Teav, T., Christen, S., Di Conza, G. et al.**, alpha-ketoglutarate orchestrates macrophage activation through metabolic and epigenetic reprogramming. *Nat. Immunol.* 2017. **18**: 985–994.

25 **Yoon, B. R., Oh, Y. J., Kang, S. W., Lee, E. B. and Lee, W. W.** Role of SLC7A5 in metabolic reprogramming of human monocyte/macrophage immune responses. *Front. Immunol.* 2018. **9**: 53.

26 **Gaskill, P. J., Carvallo, L., Eugenin, E. A. and Berman, J. W.** Characterization and function of the human macrophage dopaminergic system: implications for CNS disease and drug abuse. *J Neuroinflammation*. 2012. **9**: 203.

27 **Erlich, J. R., To, E. E., Luong, R., Liong, F., Liong, S., Oseghale, O., Miles, M A. et al.**, Glycolysis and the pentose phosphate pathway promote LPS-induced NOX2 oxidase- and IFN-beta-dependent inflammation in macrophages. *Antioxidants (Basel)*. 2022. **11**: 1488.

28 **Ruggeri Barbaro, N., Van Beusecum, J., Xiao, L., do Carmo, L., Pitzer, A., Loperena, R., Foss, J. D. et al.**, Sodium activates human monocytes via the NADPH oxidase and isolevuglandin formation. *Cardiovasc. Res.* 2021. **117**: 1358–1371.

29 **Park, H. S., Jung, H. Y., Park, E. Y., Kim, J., Lee, W. J. and Bae, Y. S.** Cutting edge: direct interaction of TLR4 with NAD(P)H oxidase 4 isozyme is essential for lipopolysaccharide-induced production of reactive oxygen species and activation of NF-kappa B. *J. Immunol.* 2004. **173**: 3589–3593.

30 **Sardenberg, C., Suassuna, P., Watanabe, R., Cruz Andreoli, M. C., Aparecida Dalboni, M., Faria Seabra, V., Draibe, S. A. et al.**, Balance between cytokine production by peripheral blood mononuclear cells and reactive oxygen species production by monocytes in patients with chronic kidney disease. *Ren. Fail.* 2004. **26**: 673–681.

31 **Gazendam, R. P., van de Geer, A., van Hamme, J. L., Helgers, L., Rohr, J., Chrabieh, M., Picard, C. et al.**, Proinflammatory cytokine response toward fungi but not bacteria in chronic granulomatous disease. *J. Allergy Clin. Immunol.* 2016. **138**: 928–930 e4.

32 **Chanteux, H., Guisset, A. C., Pilette, C. and Sibille, Y.** LPS induces IL-10 production by human alveolar macrophages via MAPKinases- and Sp1-dependent mechanisms. *Respir. Res.* 2007. **8**: 71.

33 **Tone, M., Powell, M. J., Tone, Y., Thompson, S. A. and Waldmann, H.** IL-10 gene expression is controlled by the transcription factors Sp1 and Sp3. *J. Immunol.* 2000. **165**: 286–291.

34 **Wen, A. Y., Sakamoto, K. M. and Miller, L. S.** The role of the transcription factor CREB in immune function. *J. Immunol.* 2010. **185**: 6413–6419.

35 **Ryu, H., Lee, J., Zaman, K., Kubilis, J., Ferrante, R. J., Ross, B. D., Neve, R. et al.**, Sp1 and Sp3 are oxidative stress-inducible, antideath transcription factors in cortical neurons. *J. Neurosci.* 2003. **23**: 3597–3606.

36 **Kumashiro, N., Tamura, Y., Uchida, T., Ogihara, T., Fujitani, Y., Hirose, T., Mochizuki, H. et al.**, Impact of oxidative stress and peroxisome proliferator-activated receptor gamma coactivator-1alpha in hepatic insulin resistance. *Diabetes*. 2008. **57**: 2083–2091.

37 **Ichiki, T., Tokunou, T., Fukuyama, K., Iino, N., Masuda, S. and Takeshita, A.** Cyclic AMP response element-binding protein mediates reactive oxygen species-induced c-fos expression. *Hypertension*. 2003. **42**: 177–183.

38 **Yazdanbakhsh, M., Kremsner, P. G. and van Ree, R.** Allergy, parasites, and the hygiene hypothesis. *Science*. 2002. **296**: 490–494.

39 **Pfefferle, P. I., Keber, C. U., Cohen, R. M. and Garn, H.** The hygiene hypothesis - learning from but not living in the past. *Front Immunol.* 2021. **12**: 635935.

40 **Frankenberger, M., Pechumer, H. and Ziegler-Heitbrock, H. W.** Interleukin-10 is upregulated in LPS tolerance. *J. Inflamm.* 1995. **45**: 56–63.

41 **Ferreira, B. L., Sousa, M. B., Leite, G. G. F., Brunialti, M. K. C., Nishiduka, E. S., Tashima, A. K., Van Der Poll, T. et al.**, Glucose metabolism is upregulated in the mononuclear cell proteome during sepsis and supports endotoxin-tolerant cell function. *Front. Immunol.* 2022. **13**: 1051514.

42 **Santos, S. S., Carmo, A. M., Brunialti, M. K., Machado, F. R., Azevedo, L. C., Assuncao, M., Trevelin, S C. et al.**, Modulation of monocytes in septic patients: preserved phagocytic activity, increased ROS and NO generation, and decreased production of inflammatory cytokines. *Intensive Care Med Exp*. 2016. **4**: 5.

43 **Cheng, S. C., Scicluna, B. P., Arts, R. J., Gresnigt, M. S., Lachmandas, E., Giamarellos-Bourboulis, E. J., Kox, M. et al.**, Broad defects in the energy metabolism of leukocytes underlie immunoparalysis in sepsis. *Nat. Immunol.* 2016. **17**: 406–413.

44 **Widdrington, J. D., Gomez-Duran, A., Pyle, A., Ruchaud-Sparagano, M. H., Scott, J., Baudouin, S. V., Rostron, A J. et al.**, Exposure of monocytic cells to lipopolysaccharide induces coordinated endotoxin tolerance, mitochondrial biogenesis, mitophagy, and antioxidant defenses. *Front. Immunol.* 2018. **9**: 2217.

45 **Temba, G. S., Kullaya, V., Pecht, T., Mmbaga, B. T., Aschenbrenner, A. C., Ulas, T., Kibiki, G. et al.**, Urban living in healthy Tanzanians is associated with an inflammatory status driven by dietary and metabolic changes. *Nat. Immunol.* 2021. **22**: 287–300.

46 **Dai, Z., Ramesh, V. and Locasale, J. W.** The evolving metabolic landscape of chromatin biology and epigenetics. *Nat. Rev. Genetics*. 2020. **21**: 737–753.

47 **Cavalli, G. and Heard, E.** Advances in epigenetics link genetics to the environment and disease. *Nature*. 2019. **571**: 489–499.

48 **Smolen, K. K., Cai, B., Fortuno, E. S. R., Gelinas, L., Larsen, M., Speert, D. P., Chamekh, M. et al.**, Single-cell analysis of innate cytokine responses to pattern recognition receptor stimulation in children across four continents. *J. Immunol.* 2014. **193**: 3003–3012.

49 **Fuhrer, T., Heer, D., Begemann, B. and Zamboni, N.** High-throughput, accurate mass metabolome profiling of cellular extracts by flow injection-time-of-flight mass spectrometry. *Anal. Chem.* 2011. **83**: 7074–7080.

Abbreviations: **2-ME**: 2-methoxyestradiol · **6-AN**: 6-aminonicotinamide · **DPI**: diphenyleneiodonium chloride · **ECAR**: extracellular acidification rate · **FDR**: false discovery rate · **G6PD**: glucose-6-phosphate dehydrogenase · **MQ**: mitoquinone · **NAC**: N-acetyl-cysteine · **OCR**: oxygen consumption rates · **OXPHOS**: oxidative phosphorylation · **PBMCs**: peripheral blood mononuclear cells · **PPP**: pentose phosphate pathway · **SOD**: superoxide dismutase

Full correspondence: Bart Everts and Maria Yazdanbakhsh, Leiden University Center of Infectious Diseases, Albinusdreef 2, 2333 ZA Leiden, the Netherlands
e-mail: m.yazdanbakhsh@lumc.nl; b.everts@lumc.nl

Received: 23/1/2024
Revised: 3/6/2024
Accepted: 4/6/2024
Accepted article online: 7/6/2024

© 2024 The Author(s). *European Journal of Immunology* published by Wiley-VCH GmbH.

15214141, 2024, 9, Downloaded from https://onlinelibrary.wiley.com/doi/10.1002/eji.202451029, Wiley Online Library on [24/04/2025]. See the Terms and Conditions (https://onlinelibrary.wiley.com/terms-and-conditions) on Wiley Online Library for rules of use; OA articles are governed by the applicable Creative Commons License